~~Using~~ Exploring how Sentinel-1 wet snow maps ~~to~~ can inform fully-distributed physically-based snowpack models

Bertrand Cluzet[1], Jan Magnusson[1], Louis Quéno[1], Giulia Mazzotti[2,1], Rebecca Mott[1], and Tobias Jonas[1]

[1]WSL Institute for Snow and Avalanche Research SLF, Davos, Switzerland
[2]Univ. Grenoble Alpes, Université de Toulouse, Météo-France, CNRS, CNRM, Centre d'Études de la Neige, Grenoble, France

Correspondence: Bertrand Cluzet (bertrand.cluzet@slf.ch)

Abstract. Distributed energy and mass-balance snowpack models at sub-kilometric scale have emerged as a tool for snow-hydrological forecasting over large areas. However, their development and evaluation often rely on a handful of well observed sites on flat terrain with limited topographic representativeness. Validation of such models over large scales in rugged terrain is therefore necessary. Remote sensing of wet snow has always been motivated by its potential utility in snow hydrology. However, its concrete potential to enhance physically based operational snowpack models in real time remains unproven. Wet snow maps could potentially help refining the temporal accuracy of simulated snowmelt onset, while the information content of remotely sensed snow cover fraction pertains predominantly to the ablation season. In this work, wet snow maps, derived from Sentinel-1 and snow cover fraction (SCF) retrieval from Sentinel-2 are compared against model results from a fully distributed energy-balance snow model (FSM2oshd). The comparative analysis spans the winter seasons from 2017 to 2021, focusing on the geographic region of Switzerland. We use the concept of wet snow line (WSL) to compare Sentinel-1 wet snow maps with simulations. We show that while the match of the model with flat-field snow depth observation is excellent, the WSL reveals ~~insufficient~~ a delayed snow melt in the southern aspects. Amending the albedo parametrization within FSM2oshd allowed achieving earlier melt in such aspects preferentially, thereby reducing WSL biases. Biases with respect to Sentinel-2 snow line (SL) observations were also substantially reduced. These results suggest that wet snow maps contain valuable real-time information for snowpack models, nicely complementing flat-field snow depth observations, particularly in complex terrain and at higher elevations. The persisting correlation between wet snow line and snow line biases provides insights into refined development, tuning and data assimilation methodologies for operational snow-hydrological modelling.

1 Introduction

Seasonal snow is crucial for the hydrology of mountains and their tributaries as it stores wintertime precipitation and entails
delayed runoff (Barnett et al., 2005). Snowmelt runoff is key for downstream agriculture (Qin et al., 2020) and hydropower
production (Gaudard et al., 2014). Intense snowmelt can also lead to dramatic floods (Diffenbaugh et al., 2013). As the inter-
annual variability of snow distribution is high, anticipating the amount and timing of melt is therefore essential, especially in a
changing climate (Lafaysse et al., 2014).

Snow models have therefore become indispensable in the field of hydrological forecasting (e.g. Griessinger et al., 2019).
However, accurately resolving all intricate processes that influence the mass and energy balance of the snowpack across various
spatial scales is difficult. The accumulation of snow in a region is contingent upon precipitation patterns, which exhibit substan-
tial variability both regionally (Isotta et al., 2014) and locally (Scipión et al., 2013). Wind and gravitational redistribution con-
tribute to the spatial heterogeneity of snowpacks ~~(Liston and Sturm, 1998; ?; Mott et al., 2018)~~(Liston and Sturm, 1998; Freudiger et al., 20
. Meanwhile, the surface energy balance, which governs the amount of snowmelt, is subject to fine-scale variations. These vari-
ations are influenced by topographical features and cloud cover, which impact incoming shortwave and longwave radiation
(Brauchli et al., 2017; Jonas et al., 2020) as well as air temperature. Wind patterns, too, can exert influence on sensible and
latent heat fluxes at small scales (Mott et al., 2011). In summary, the accurate modelling of snowpack ablation necessitates the
comprehensive representation of both the variability in snow cover and the multifaceted drivers affecting its energy balance.

Snow melt is not equivalent to snowmelt runoff. Snowmelt runoff can only commence when meltwater exits the snowpack
from its bottom. This journey entails complex processes related to liquid water storage and routing, introducing a substantial
temporal lag between the initiation of melt and eventual snowmelt runoff (Lundquist and Dettinger, 2005). Towards the end
of the accumulation season, an increase of the surface energy input typically gives rise to more frequent and intense episodes of
surface melt, a phase often referred to as the moistening phase (Techel and Pielmeier, 2011; Dingman, 2015; Marin et al., 2020)
. Concurrently, rainfall events may further augment the liquid water content at the surface. Once the amount of liquid water in
the upper layers of the snowpack reach ~~saturation, liquid water gradually infiltrates through the snowpack during the ripening phase~~the maximum holding capacity, the liquid water released or absorbed from the superficial layers gets in contact with the
subfreezing snow present underneath and freezes. This releases latent heat that causes the snowpack to warm up. This starts
the process of snow ripening. This drainage process is influenced by various factors, including refreezing, the presence of
preferential flow paths, ~~and capillary barriers~~capillary barriers, and lateral flow (Wever et al., 2014; Würzer et al., 2017), as
well as the occurrence of ice layers (Quéno et al., 2020). Ultimately, snowmelt runoff commences when the liquid water exits
the snowpack at its base.

In the context of large scale and high spatial resolution snowmelt applications, compromises are needed to find a good
trade-off between model accuracy and computational costs. Often, intermediate-complexity snowpack models provide a good

balance (Magnusson et al., 2015). These models solve the energy and mass balance of the snowpack with simplifications as to the representation of the internal snowpack structure (Marsh et al., 2020; Essery, 2015). Particularly, they use a limited number of numerical layers (Cristea et al., 2022) resulting in a simplified description of liquid water routing and snow metamorphism.

55 These factors, combined with further uncertainties in meteorological forcings, may result in considerable modelling errors (Raleigh et al., 2015; Krinner et al., 2018), which are often hard to assess because of an intrinsic lack of observational data in mountainous areas.

Satellite observations of the snowpack could help to constrain such model errors, provided that they have the adequate spatio-
60 temporal resolution and sufficient accuracy (Largeron et al., 2020). Snow cover fraction (SCF) observations from Sentinel-2, for instance, are available at a resolution of 20m every three to five days, however only in the absence of clouds. The C-band synthetic aperture radar (SAR) sensor on Sentinel-1, on the other hand, is sensitive to the presence of liquid water in the snowpack irrespective of cloud cover (Veyssière et al., 2019; Marin et al., 2020; Karbou et al., 2021). Binary wet snow maps (WSM) can be derived from SAR backscatter at a resolution higher than 100m, requiring only small amounts of liquid water for snow
65 to be classified as wet (Nagler et al., 2016).

The timing of information is key in real-time operational modelling. Snow cover fraction and wet snow maps provide information at different times during the season. SCF observations provide information about the first snowfall, and during the period of partial snow cover during the ablation season. This information can be used to reconstruct snow water equivalent
70 ~~(Margulis et al., 2016)~~through data assimilation (e.g. Margulis et al., 2016; Fiddes et al., 2019), but is not helpful for determining the onset of snowmelt in real-time (Andreadis and Lettenmaier, 2006; Buchelt et al., 2022). Wet snow retrievals, on the other hand, provide qualitative information during the onset of snowmelt, leaving the entire ripening and ablation phase to exploit the information. ~~Key to operational snow-hydrological model applications, wet snow retrievals can anticipate the onset of snowmelt, making them a potentially interesting data source for assimilation (Malnes et al., 2015).~~

75

Nevertheless, several questions remain as to the potential utility of wet snow maps in this context. Firstly, the SAR signal may ~~capture~~ detect superficial short-lived melt events which are very difficult to capture by intermediate-complexity snowpack models. These models do not ~~capture~~ represent the intricate microstructure and stratigraphy of the snow, thereby complicating the assimilation process. The duration of the ripening phase, associated with the delay between the SAR signal and the onset
80 of snowmelt runoff, is also arguably very variable, depending on the snowpack thickness, internal properties, and springtime weather conditions (Marin et al., 2020). Finally, due to the sensitivity of radar retrievals to seasonal change in land surface properties (Karbou et al., 2022) and the unavailability of meaningful retrievals in forested areas, reliable observations are confined to elevations above the treeline and away from water bodies and human activities.

85 In this work, we assess whether information from wet snow maps can be used to inform a snow hydrological model used in nationwide operational forecasting in practice. We use two versions of our physically-based multi-layer snowpack model

FSM2oshd (Mott et al., 2023), which we run operationally over entire Switzerland at 250m spatial resolution. These two versions have different fresh snow albedo parametrizations. Snow depth data from nearly 450 monitoring stations were assimilated into these simulations, to ensure a good model performance free of systematic overall biases to start with. Note that this approach was chosen to reveal the value of information contained in WSM and SCF products beyond the identification and removal of obvious model biases. The study focuses on five ablation seasons (March-July) from 2017 to ~~2021 addressing the following questions:~~

- ~~Is information from Sentinel-2 snow cover fraction and Sentinel-1 wet snow complementary to already available flat field snow depths?~~

- ~~Is it possible to leverage remotely sensed data on wet snow to enhance the accuracy of snowpack simulations in complex terrain?~~

2021. The study area, observations and modelling chain are described in Sec. 2. The results are presented and discussed in Sec. 3 & 4. We finally conclude and open research perspectives in Sec. 5.

2 Material and methods

2.1 Study area

The study area encompasses Switzerland and hydrologically connected areas outside its boundaries (see Fig. 1). The domain size stretches over 272km in the latitudinal direction and 365km in the longitudinal direction, ~~totalling~~ totaling 920,884 model grid cells at a resolution of 250m. We focus our analysis on 16 ~~hydrological units (MEZ~~subcatchments with relatively homogeneous snow conditions ("MEZ", as defined by the Swiss federal office of environment), which cover the alpine area of the domain. The average size of the MEZs is about 1600km^2, ranging from 721km^2 (MEZ 16) and 4470km^2 (MEZ 9). All of these units are located within Switzerland, some of them extending to neighbouring countries (Liechtenstein, Austria, Germany, Italy, and France). The MEZs are situated on both sides of the main alpine ridge and encompass diverse hydro-climatic conditions.

There are 444 locations with daily in-situ snow depth observations measured on a flat surface available throughout the domain indicated by the red dots in Figure 1. Among these observations, 255 are within the considered MEZs.

2.2 Satellite observations from AlpSnow

AlpSnow is a project from the European Spatial Agency (ESA) which provides a 5-year demonstration dataset for novel remote-sensing retrievals of snow parameters over the Alps. In this paper, we use a wet snow maps product, retrieved from Sentinel-1 and snow cover fraction from Sentinel-2.

2.2.1 Wet Snow

Wet snow maps from AlpSnow are processed from Sentinel-1 C-band synthetic aperture radar backscatter time series. C-band backscatter is sensitive to small amounts of liquid water in the snowpack, causing a sharp decrease in backscatter compared to bare ground or dry snow conditions (Mätzler, 1987). A -2.5dB threshold with respect to a reference scene is applied to detect wet snow, resulting in binary wet snow maps (Nagler et al., 2016). As evidenced by Marin et al. (2020), the backscatter signal resumes to dry snow conditions as the snowpack becomes patchy throughout the ablation season, even though at that time the snowpack ~~is usually fully~~ column is usually entirely saturated with liquid water. Therefore, melting, patchy snow cannot be distinguished from dry snow or bare ground. Furthermore, in snow-free conditions, spurious backscatter drops may be caused land surface change (e.g. vegetation growth and agriculture), changes in soil wetness, and speckle noise (e.g. Guiot et al., 2023), resulting in false wet snow classification. For this reason, the wet snow detection algorithm from AlpSnow includes a snow mask computed from a gap-filled, temporally interpolated remotely-sensed snow cover product. Any pixel with 40% or less snow cover fraction is considered as snow-free. Furthermore, due to the ~~viewing slant angle~~ slant angle under which SAR acquisition is performed, geometric distortions (~~shadows,~~ layover and foreshortening) ~~cause~~ as well as shadowing result in data gaps in rugged terrain. The product has therefore the three following classes: wet snow, snow-free or dry snow or patchy snow, and masked pixels. Satellite acquisition occurs around 5UTC (descending orbit) or 17UTC (ascending orbit) with a revisit time of 3 to 6 days during the study period (see Fig. 2a-b). AlpSnow wet snow maps resolution is 0.001^ox0.001^o in WGS84 (EPSG:4326) corresponding to approximately 100mx100m in the modelling coordinate system (EPSG:21781).

Wet snow maps were aggregated into pixels of 250m ~~coinciding with~~ corresponding to the cells of the model grid. Products were first reprojected and resampled at 50m using a nearest neighbour approach into the modelling coordinate system. Then, these products were masked using a 10m forest mask (Mott et al., 2023) which is more accurate than the forest mask used in the raw data. Urban areas were also excluded using class 50 of the Copernicus Land Cover Mask (Buchhorn, 2022). For each 250m pixel, an aggregated binary value was computed from the twenty five 50m subpixels as follows:

- If more than 90% of the 50m-subpixels were forest/urban, then the pixel was masked as forest/urban.

- Else, if more than 5% of the 50m-subpixels were classified as geometric distortions, then the pixel was masked out.

- Otherwise, the 250m wet snow binary value was equal to the majority of the valid subpixel values.

Fig. 2a and b show that due to overlapping tracks, 5 to 10 Sentinel-1 wet snow observations were available per month. Some areas (MEZ 6, 14, 17 and 22) are even observed ten times a month in the morning and evening.

2.2.2 Snow Cover Fraction

AlpSnow snow cover fraction is derived by spectral unmixing on Sentinel-2 level 1C radiance at the pixel level (Keuris et al., 2023). Product resolution is 0.0002^ox0.0002^o in WGS84 (EPSG:4326), (approximately 20mx20m in EPSG:21781). Satellite acquisition time is around 10–11h UTC. The following Sentinel tiles were processed: 'T31TGM', 'T32TMT', 'T32TNT',

'T32TLS', 'T32TMS', 'T32TNS'. Based on optical data, these products are inherently ~~limited~~ affected by the following ~~factors~~ problems (e.g. Barrou Dumont et al., 2021; Keuris et al., 2023):

- ~~cloud/snowdiscrimination,~~ it is difficult to discriminate clouds from snow, and to delineate cloud shadows

- ~~missed detection of cirrus clouds~~ undetected thin cirrus clouds may cause a decrease of the retrieved snow cover fraction

- shaded snow in steep terrain and sparse forests, may also be affected by negative biases in SCF, in particular from November to March ~~,~~ when shadow extents are larger (and there is snow on the ground)

- ~~non-zero snow cover fraction attributed to~~ non discrimination of snow and bare ice, causing snow-free glaciers ~~, usually in Summer~~ to be classified as snow.

We mitigate these limitations by focusing on observations available in open terrain, in the ablation season from April to June.

SCF images were aggregated following a similar procedure as for the WSM (see Sec. 2.2.1). Products were reprojected and ~~and~~ resampled at 10m. For each 250m pixel, an aggregated value was computed as follows:

- if more than 90% of the 10m-subpixels were forest/urban, then the pixel was masked as forest/urban.

- else, if more than 5% of the 10m-subpixels were covered by clouds, the the pixel was masked as cloudy.

- otherwise, the 250m SCF value was computed as the average value of the valid (non forested, urban or cloudy) subpixels.

Fig. 2c shows the average value of valid Sentinel-2 SCF observations per pixel during the spring period from April to June (thereby accounting for cloud occurrence). Due to overlapping tracks, the central portion of the domain, covering MEZ 6, 11, 18, 20 and 22 has twice as many Sentinel-2 overpasses as the rest of the domain. On average, 2 to 5 cloud-free observations are available per pixel each month.

2.3 FSM2oshd

In this work, we use the physically-based multi-layer snowpack model FSM2oshd (Mott et al., 2023), which we run operationally over entire Switzerland at 250m spatial resolution. The snowpack model is run using output from the numerical weather prediction system COSMO-1E operated by MeteoSwiss, which is carefully debiased and downscaled to 250m using a range of dynamical and statistical methods. In particular, shortwave radiation is provided per inclined surface. FSM2oshd includes an optimal-interpolation based data assimilation scheme, using in-situ snow depth measurements from 444 stations (see Fig. 1) to correct for snowfall input errors (Magnusson et al., 2014). To account for unrepresented preferential deposition, wind transport, and gravitational redistribution of snow, a terrain-dependent correction is applied to solid precipitation based on Vögeli et al. (2016). In its standard configuration, FSM2oshd is a 3-layer snowpack model where liquid water routing through the snowpack is modelled using a bucket approach.

A subgrid parametrization is used to derive pixel-level snow cover fraction from seasonal values of SWE and HS ~~, accounting for~~ (Helbig et al., 2021). This model component accounts for the impact of subpixel terrain roughness and ~~recent snowfall history (Helbig et al., 2021). This is an essential component when it comes to comparing~~ slope variability on snowdepth distribution at the peak of accumulation. For instance, smooth and flat pixels usually exhibit homogeneous subpixel SWE distribution, leading to a more rapid reduction in snow cover as SWE decreases. Fresh snow events are assumed to produce abrupt yet transient increases in snow cover fraction. Accounting for this is essential to compare model output with satellite retrievals of snow cover fraction ~~. The snowpack model is run using output from the numerical weather prediction system COSMO-1E operated by MeteoSwiss, which was carefully debiased and downscaled to 250using a range of dynamical and statistical methods. More details about FSM2oshd are available in Mott et al. (2023), describing in-depth the entire modelling framework including preprocessing of input data and available data assimilation schemes~~at this scale.

FSM2oshd uses a re-calibrated version of the albedo parameterization from Douville et al. (1995) and Essery et al. (2013). In the parameterization, the snowpack albedo decays linearly with time when the snow surface temperatrure is below zero °C and decays exponentially when the surface is melting. The minimal albedo value is 0.5. The constant decay times scales are $\tau_{melt} = 130$h for melting snowpack surface, and $\tau_{cold} = 3000$h for subfreezing surface temperature, reflecting the fact that wet snow metamorphism is quicker than dry snow metamorphism. In the presence of snowfall, the albedo is progressively refreshed to fresh snow values.

~~Here, we use two versions of FSM2oshd: a)the pre-operational version fsm_preop was configured to match snow depth observations from several Swiss monitoring networks, mostly at flat unforested measuring sites.~~In FSM2oshd, the fresh snow albedo α_{fs} varies as a function of altitude z as follows:

$$\alpha_{fs} = \begin{cases} 0.8, & \text{if } z <= 1500 \\ \alpha_{fs}^{max} + \frac{2300-z}{2300-1500}(0.8 - \alpha_{fs}^{max}), & \text{if } 1500 < z <= 2300 \\ \alpha_{fs}^{max}, & \text{otherwise} \end{cases} \tag{1}$$

The snowpack albedo α increases with hourly snowfall Sf(mm):

$$\alpha = \begin{cases} \alpha_{fs} & \text{if } Sf_{24h} > Sf_{min} \\ \alpha + (\alpha_{fs} - \alpha)\frac{Sf}{Sf_{min}}, & \text{otherwise} \end{cases} \tag{2}$$

This rule includes a threshold enforcing an albedo of α_{fs} for 24h-snowfall above $Sf_{min} = 10$mm (Douville et al., 1995). The albedo parameterizations in fsm_preop ~~, however, was not tuned in any way using spatially fully-distributed datasets, such as remote sensing products; b) the version fsm_optim was optimized to address a model deficiency detected in~~ were tuned through an assessment against snow depletion rates in springtime measured t flat field sites (Mott et al., 2023), where α_{fs}^{max} was set to 0.92. A preliminary comparison with Sentinel-1 wet snow retrievals (c.f. Sec ~~. 3.2). The optimization consisted~~

of lowering the fresh snow albedo 3.2), however, showed that in fsm_preop simulations melting was initiated too late with a particular focus in the south-exposed slopes. As we will show, this model shortcoming could be mitigated by lowering α_{fs}^{max} from 0.92 in fsm_preop to 0.86 in the so-called fsm_optim , to accelerate the onset of snowmelt particularly in south facing aspects version. Below, we will compare both model versions.

2.4 Comparing the model with observations

In order to compare the simulations with observations, model outputs were extracted and masked out when the forest fraction exceeded 80% of the grid cell. The same mask was applied to the observations, to avoid strong geospatial bias in the analysis. The definition of a "wet snow" state for the model is required for a direct comparison with the observations. Given the high sensitivity of the observation to small liquid water amounts in the snowpack, we considered modelled snow to be wet as soon as liquid water was present in any of the snow layers the total liquid water content was strictly above zero at the time of the acquisition (either 05UTC or 17UTC).

2.5 Deriving the Wet Snow line

The melting season usually starts with a progressive moistening of the dry snowpack from low to high elevations. The wet snow line (WSL) is the time-varying elevation of this wetting front (Gupta, 2011), which primarily also depends on topographic factors such as aspect and slope. As shown by Karbou et al. (2021, 2022), wet snow maps from Sentinel-1 capture this phenomenon well. The WSL is conceptually very similar to the snow line (SL), which can be defined as the elevation where the snow cover fraction equals 50% (e.g. Parajka et al., 2010).

The WSL was estimated from Sentinel-1 wet snow maps and "wet snow" states from model outputs (Sec. 2.4) using the following algorithm. Using the MEZs as spatial aggregation units, we computed the WSL by aspect sectors each time a Sentinel-1 image was available. Pixels with a slope $< 8^o$ were considered as flat, and pixels above 30° of slope were excluded from the aggregation. Only data between 1600 and 3200 ma.s.l. were evaluated, to enable a robust estimation of WSL unaffected by forests and high-elevation glacierized areas (see Sec. 2.2.1). All valid pixels in a given aspect were stratified by elevation. We then computed a weighted interpolation of the pixel values using a window width of 300m of elevation giving us the proportion of wet pixels (Wet Snow Fraction, WSF) as a function of the elevation as shown in Fig. 3. Note that towards low elevations, Alpsnow observed wet snow fraction is decreasing probably because of snow roughness and a decreasing snow cover fraction.

For the observations, starting from dry conditions at high elevations we identify the maximum WSF_{max} as we go to lower elevations. If WSF_{max} did not exceed 0.6, then the snowpack was not substantially wet, and no snow line was determined for that aspect class. Otherwise, the WSL was defined as the lowest elevation above that of WSF_{max} with a $WSF <= 0.8 \times WSF_{max}$. If this value was This value was determined manually. If it was not reached, the snow cover was assumed to be wet over the entire elevational range considered, and no WSL was determined either.

The snow line (SL) was computed using the same weighted interpolation to arrive at an elevational profile of SCF. The SL was then defined as the highest elevation with $SCF < 0.5$.

3 Results

3.1 Performance of the snow model against flat-field observations

Fig. 4 shows the performance of both FSM versions, fsm_preop and fsm_optim against flat field observations between 2000 and 2500 m a.s.l. across Switzerland for the five considered years. Overall, the match is excellent, in particular during the accumulation period, which is consistent with the fact that these observations were assimilated for correcting errors in the snowfall input (see Sec. 2.3). For a detailed evaluation of FSMoshd against station data, readers are referred to (Winstral et al., 2019; Mott et al., 2023; Obe . For both model versions, the most notable differences with respect to the observations arise in the early ablation period, in particular during spring 2019 and 2021. As expected, due to a slightly lower fresh snow albedo, snow melt is initiated slightly earlier in fsm_optim compared to fsm_preop. Aimed mostly at south facing slopes, the ~~optimisation~~ optimization had only limited influence on simulations at our flat field monitoring sites. The accelerated melt, however, leads to slightly stronger negative biases, albeit within acceptable limits. This is particularly notable in seasons when fsm_preop already demonstrates a slight negative bias, such as in the winter years of 2019 and 2021.

3.2 Spatial comparison and topographic aggregation of satellite observations

Satellite data provide much more information on the spatial performance of the model than the station dataset. As an example, Fig. 5 shows the wet snow map aggregated to the model resolution of 250m compared with equivalent model simulations with fsm_preop for MEZ 11 on 1st April 2019. Both simulated and observed maps are dry at high elevations, and transition into wet conditions at lower elevations. In the ~~south~~ South-facing slopes, the observations indicate wet conditions ~~up to higher elevations~~ several hundred meters higher than the model simulation. No retrieval is available in some steep slopes of the South West aspect due to geometric distortions (shadowing) of the SAR signal.

In order to gain quantitative insights into the spatial dynamics of wet snow in both observations and model, map products were aggregated by slope classes in Fig. 6, including respective evaluations of the wet snow line. Observations (Fig. 6a) and fsm_preop (Fig. 6b) show good agreement in the northern sectors as well as in flat terrain. However, in the South-West to East slopes, the simulated WSL consistently shows notably lower values compared to the observations (as also observed in Fig. 5). This suggests a delayed initiation of simulated snow melt in sun-exposed terrain. This finding led to testing whether lowering the fresh snow albedo would mitigate existing model biases by enabling an earlier onset of melt preferentially in sun exposed slopes, motivating the parameter adaptation applied in fsm_optim. Indeed, simulations of the wetting front with fsm_optim

270 (Fig. 6c) show a substantially better match to observations, particularly in West and South aspects, but also for flat terrain, with a raise in the WSL by up to 300m relative to the baseline simulations with fsm_preop.

3.3 Time series of snow line and wet snow line

Generalizing the approach, both WSL and SL were computed over the course of the melt season, for all MEZs, and all years. Results for MEZ 11 on descending orbits (05 UTC) are shown in Fig. 7. Results for ascending orbits (17 UTC) can be found

275 in Fig. A1. Using fsm_preop, we see in the upper panel of Fig. 7 that the wet snow line gradually rises to high elevations from March to May each year, both in the observations and in the model(Fig. 7, left). From June onwards (and even May in 2018 and 2020), the snowpack is wet up to high elevations and no WSL can be defined, i.e. the signal is saturated both in the observations and the model. In the North sector, the match between observations and simulations is good, except in 2017 where the model shows a considerably delayed onset of melt for elevations between 2200m and 2400m. Southerly exposures, characterized by

280 significant inter-annual variability, the model consistently exhibits a prolonged delay throughout the season. The simulated wet snow tends to be frequently positioned about 300m lower than observed values. From April onwards, fsm_optim shows a higher WSL than the fsm_preop version, usually by 200 to 300m. The match with observations is therefore better, in particular in the South exposed slopes.

285 Compared to the assessment of the WSL, the SL time series show a much better agreement between observations and simulations than the WSL (Fig. 7, right). The agreement between observations and fsm_preop is particularly good in the Northerly slopes and in flat terrain, for almost all years. However some expositions show a too high snow line for the model (e.g. flat in 2018), and the snow line is most of the times too low in the South sector (years 2017, 2020 and 2021 in particular). The SL of fsm_optim becomes significantly higher (100–200m) than that of fsm_preop from mid-May onwards. This results in an overall

290 better match with the observations, with some exceptions (flat exposition in 2018 for example).

Comparing both WSL and SL products, we note that the years with the lowest SL bias for fsm_preop seem to coincide with the strongest WSL biases for that model version. Moreover, for a given elevation, there is a fairly consistent time lag between the WSL and the SL of one to two months.

295

3.4 Relationship between spring seasonal biases of WSL and SL

The time series of Fig. 7 show a persistence of WSL biases in fsm_preop across the entire season, suggesting a potential correlation with SL biases. In essence, our hypothesis posits that a delayed onset of melt in the model will likely lead to a delayed melt-out. To confirm this hypothesis, we conducted an analysis by computing the average model WSL bias and SL bias per

300 year (over March-May and April-June, respectively), aspect and MEZ. Fig. 8a shows results for fsm_preop for all five years, all aspects, and MEZ 11. Overall, some correlation ($R^2 = 0.32$) can be observed between the WSL and the SL biases, where often fsm_preop is too dry coinciding with overestimated snow cover extent. WSL biases, however, are much higher in amplitude

than SL biases (around -500–0m, vs -200–100m respectively). The biases vary both between years and aspect classes. For instance, 2021 exhibits overall strong biases, while 2018 is almost unbiased. The year 2019 stands out from the other years featuring a slightly higher SL bias. This anomaly is likely due to a single fresh snow event in May during which the snow line was several hundred meters too high in the model (Fig. 7). Within each year, the WSL bias for fsm_preop is dominated by a North-South contrast. While the northern slopes (upwards pointing triangle) typically exhibit the least negative biases, southern slopes (downwards pointing triangle) exhibit the most negative biases, in the range of -500m to -200m. Similarly, the SL biases feature a North-East (square) to South-West (pentagram) contrast. This results in a very specific pattern: for each year, as we circle through the expositions clockwise, the bias values draw an ellipse anti-clockwise.

The predominant factor contributing to the North-South disparity in ablation is likely the shortwave radiative input. Expectedly, a lower fresh snow albedo value, as implemented in fsm_optim (see Sec. 2.3), could therefore induce an earlier melt in the model, while at the same time enhancing differential melting dynamics between North and South faces. Results with fsm_optim show considerably reduced biases (Fig. 8b). Overall, with fsm_optim biases are better ~~centred~~ centered around zero, while the range of biases between aspects for any given year are reduced, particular with regards to WSL biases. The correlation between biases in WSL and SL is also reduced from 0.32 to 0.13. Yet, the overall biases continue to vary between years. For instance, fsm_optim under-predicts both WSL and SL in 2021, while predominantly over-predicting WSL and SL in the year 2018. These results also stand when considering all the years and MEZ (Fig. 9). Despite the noticeable fluctuations between years, it is noteworthy that biases in WSL are considerably lower with fsm_optim compared to fsm_preop. This reduction also aligns with a significant decrease in the negative bias observed in SL.

4 Discussion

4.1 On the proposed wet snow line metric

In this study, we have evaluated the potential of Sentinel-1 based wet snow maps for the performance assessment of snow-hydrological models in the ablation period. Leveraging the wet snow line concept facilitated a robust analysis of the information provided by Sentinel-1 wet snow maps for high spatial resolution snowpack modelling. The topographic aggregation facilitated the direct comparison between remotely sensed observations and model simulations, while achieving a good level of robustness against individual observation errors and data gaps as done in the literature (Mary et al., 2013; Karbou et al., 2022). Topographic aggregation makes the analysis more robust to missing or erroneous data in the observations, which is particularly important in the context of data assimilation (Cluzet et al., 2021). At the same time, while some relevant information from individual pixels may be lost, key spatial information were maintained by resolving biases in terms of region, elevation, aspect, and slope, which has been shown to be of critical relevance (Cluzet et al., 2020).

Figs. 3 and 6, as well as results from Karbou et al. (2021) suggest that this topographic aggregation can be further exploited to address shortcomings of the WSL retrievals (see Sec. 2.5 and Fig. 3): if a snowpack is wet at a given altitude, it will be wet at

a lower altitude, all other things being equal. The wet snow line is therefore a condensed and potentially useful metric for both remote sensing and modelling, while the direct assimilation of binary ~~WSL or SL products~~ products such as wet snow maps (or snow masks) into physically based snow models is typically seen as unfavourable (Baba et al., 2018; De Lannoy et al., 2012).

340   ## 4.2   On the albedo correction

The wet snow line analysis evidenced a systematic dry bias in the pre-operational version of our model, fsm_preop (Fig. 8a). The ~~adjusted albedo~~ comparison of observed versus simulated WSL revealed a systematic pattern with model biases being particularly pronounced in the south exposed slopes. This pattern indicated the need for a model adaptation that would accelerate the initiation of snowmelt particularly in south-facing terrain, suggesting a mitigation strategy with focus on shortwave

345   radiation. Since FSM is driven with shortwave radiation per inclined surface (see Mott et al., 2023), any reduction of the snow albedo will preferentially augment net shortwave radiation in south-exposed slopes. Indeed, the adjusted albedo parameterization in fsm_optim~~resulted in better simulations of~~, while being closer to literature values (e.g. Gardner and Sharp, 2010), resulted in improved simulations of wet snow and snow cover fraction (Figs. 8 ~~b and 9b). In addition, the slightly reduced variability of the~~ and 9) without incurring any considerable impairment of the excellent match between observed and simulated snow depth at the

350   stations (see Fig. 4). However, due to the lack of reliable spatialized albedo data in complex terrain (Largeron et al., 2020; Lamare et al., 202 , we can only speculate that this change actually addresses a model deficiency.

Simulated WSL and SL represent the equivalent elevation of two timing variables, i.e. the first occurrence of wet snow and the melt out date. Both are a consequence of the coupled energy and mass balance equations and are affected by changes in

355   the snow albedo in the same way: a reduction of the albedo will prepone the timing of both events, entailing a mechanism why WSL and SL biases ~~(Figs. 8b and 9b) give us additional confidence in the correction of fresh snow albedo. This proves the potential of such metric to inform snowpackmodels~~are correlated. Obviously, there are other factors that contribute to model biases of each, so that such a correlation is not perfect. Apart from the energy turnover, there is also a direct link between the occurrence of wet snow and the progression of snowmelt. The occurrence of wet snow accelerates the albedo decay through

360   wet metamorphism (see Sec. 2.3), which in turn increases the net shortwave input to the snowpack.

Observations indicate that both WSL and SL simulated by fsm_preop were typically biased low. Being able to improve both by decreasing the albedo is therefore expected. Remaining SL biases (Fig. 9) call for additional model improvements, requiring complementary data to the wet snow maps exploited in this study, spatially distributed and temporally resolved data

365   of snowdepth or SWE being the most obvious choice.
Relying solely on snow cover fraction observations would have made it challenging to point out the details of the model deficiencies present in fsm_preop. Remaining bias patterns of fsm_optim (Figs. 8b, 9b and 9b) could be due to many reasons, e.g. biases in the sub-grid parametrization for snow cover fraction (see Sec. 2.3), which derives modelled SCF from modelled snow mass (Helbig et al., 2021), biases in the observations (e.g. Aalstad et al., 2020), or biases in either simulated snow

370 accumulation or melt. In this study, wet snow observations helped to disentangle the causation by pointing at a delayed melt, particularly in South-facing slopes. Further work can now focus on revealing other factors which contribute to the remaining snow line biases.

4.3 Potential for data assimilation and model development

Significant biases, reaching up to approximately -350m, persist in the modelled wet snow line for fsm_optim, (Fig. 8b). How-
375 ever, the extent to which additional information can be extracted from the observations remains uncertain. Observations are sensitive to wet snow processes occurring at the sub-grid scale which are not accounted for in the model. The model itself has a coarse vertical resolution with 3 snow layers, which may not be enough to capture small surface melt events detected by SAR (Cristea et al., 2022; Lund et al., 2022). Further, the bucket approach used to route the liquid water through the snowpack is known to generate a slightly delayed onset of snow-melt runoff (Wever et al., 2014). On the other hand, wet snow retrievals
380 are not flawless either. SAR is sensitive to even very small amounts of liquid water and may misinterpret wet soil below a dry snowpack as wet snow (Marin et al., 2020). The retrievals are further known to be problematic in the presence of fractional snow cover, and often report dry snow conditions towards melt out when this is clearly not the case (c.f. Sec 2.2). All these factors may contribute to an irreducible mismatch between observed and simulated wet snow maps, which may question the utility of wet snow maps beyond model assessment and optimization as demonstrated in this study.

385

Several factors, however, suggest that wet snow maps contain further information, valuable for model evaluation and data assimilation in an operational model setting. First, it is interesting to note that even after model tuning, inter-annual variability dominates WSL and SL bias patterns, and that their magnitudes show a strong correlation (Fig. 8). For example, the year 2018 exhibits positive biases of WSL and SL, while it is the opposite in 2021. Operational snowpack simulations are intrinsically
390 dependent on numerical weather prediction models, which show variable performance and systematic biases between years (Winstral et al., 2019). In one year, a slight error in temperature might turn a major snowfall event into rain while in another early season snowfall might be over-predicted, both causing snow model biases that will persist throughout the entire season. Such biases could be mitigated in real-time through assimilation of wet snow retrievals, since the transition from dry to wet snow happens during the season, not at the end of the season when optical remote sensing reports melt-out.

395

The potential for data assimilation of SCF has long been established, although most of the time in a reanalysis context (Margulis et al., 2015; Aalstad et al., 2018; Alonso-González et al., 2021) rather than in real time (Baba et al., 2018). As long as the snow cover fraction equals 1, the only information that can be derived is that the snow water equivalent is above a few tens of millimetres (e.g. Magand et al., 2014). This is not very informative as long as the model is not com-
400 pletely off from reality (De Lannoy et al., 2012). Fig. 7, however, frequently illustrates a persistent bias in the snow line throughout the ablation period. This pattern implies that information collected early at lower elevations, could potentially be transferred to higher elevations through data assimilation using the propagation of information (Cluzet et al., 2021; ?) (Cluzet et al., 2021; Alonso-González et al., 2023). Such an approach has the potential to enhance the overall performance

of the model.

However, this may not be the case in the absence of systematic model biases. Fig. 7 shows that once the systematic albedo bias has been fixed in fsm_optim, there is no longer a consistent snow line bias throughout the season: there is a negative snow line bias early in the season, and then a positive one later in the season. In such a context, while reanalyses may be able to find optimal trajectories once the full time series of observations has been gathered, real-time data assimilation might result in degraded performance in the late season. SCF data assimilation could nevertheless be used to correct for the instances where the modelled fresh snow line is obviously wrong, as in May 2019 (Fig. 7).

The ellipsoidal patterns of the WSL/SL biases with respect to aspect (Fig. 8) demonstrate the potential of using WSL and SL retrievals in combination as a basis for a detailed model performance diagnosis. In most MEZ, SL biases in the eastern slopes are often substantially higher than in the western slopes by 50 to 200 m. The corresponding WSL biases, however, are in the same order of magnitude. This finding suggests a deficiency in the model's representation of wind-driven snow redistribution processes. In our climate, dominated by west winds, these processes typically lead to an uneven distribution of snow between west and east exposed slopes, a phenomenon that the model currently fails to adequately represent. Such a finding may motivate better inclusion of wind redistribution processes in FSM ~~(e.g. Vionnet et al., 2021; ?; Quéno et al., 2023)~~ (e.g. Vionnet et al., 2021; Baron et al., 2024; Quéno et al., 2023) even at the considered spatial resolution of 250m.

Conversely, the wet snow line bias in our simulations is still dominated by a South-North contrast with fsm_optim (Fig. 8b). Given the strong influence of albedo on the wet snow line, we cannot exclude that further improvements are required with respect to the representation of snow albedo. Snow metamorphism, and solar angle indeed have strong effects on the albedo, which are not accounted for in the model (e.g. Gardner and Sharp, 2010), and result in topographic variability of the albedo as evidenced by satellite imagery (e.g. Mary et al., 2013; Cluzet et al., 2020). The rather simplistic temperature-dependent time decay of albedo within FSM (Essery, 2015) cannot capture these processes in adequate detail, leaving potential for mitigation by way of data assimilation.

4.4 Complementarity with flat-field snow depth observations

As evidenced by Fig. 4, fsm_preop performs remarkably well against data measured at our 444 flat field snow monitoring sites. There is little evidence and incentive that the model should be improved from this data alone. The remote sensing data reveals model shortcomings we would have remained unaware of. Wet snow maps directed us towards a possible solution of an issue that was also visible in our snow line comparisons, demonstrating the complementarity of all three datasets involved in our model performance assessment.

Additionally, flat field snow depth observations are scarce in ~~Switzerland~~ alpine regions above 2500m a.s.l. (e.g. Cluzet et al., 2022). Likewise, precipitation and air temperature measurements used to constrain meteorological input via assimilation or de-biasing are scarce above these altitudes (Isotta et al., 2014; Vernay et al., 2022). Alpine areas are also where wind redistribution

is prominent due an enhanced exposition to winds (Dujardin and Lehning, 2022), not to mention steep terrain and glaciated areas. All in all, for these high elevations, the uncertain input data and rare validation measurements is a challenge for achieving accurate snowpack simulations. Therefore, wet snow retrievals and snow cover fraction observations offer a unique opportunity to observe the snowpack where other data is typically scarce, and provide key information to improve modelling and process understanding at high elevations. Nevertheless, a limitation arises from the challenges associated with distinguishing between snow-free and snow-covered glaciers in the snow cover fraction products.

Finally, Fig. 4 shows that the significant improvements we obtain with fsm_optim in terms of WSL and SL come at the cost of slightly deteriorating the model performance at flat field snow depth stations in the ablation period. This is not necessarily a surprise. fsm_preop inherits its tuning from model versions specifically calibrated against flat-field snow depth stations (Mott et al., 2023). The performance of fsm_preop against snow depth observations already establishes high standards. Additionally, it is a well-known fact that snow depth tends to be higher in flat terrain compared to the surrounding slopes (Grünewald and Lehning, 2015), a factor accounted for in our model through a precipitation multiplier (see Sec. 2.3). Further combining satellite observations of wet snow and snow cover fraction with flat-field snow depth observations could help refining the relative behaviour of models in flat terrain with respect to the complex topography that predominates in mountain areas.

5 Conclusions

This work investigated the potential of wet snow retrievals from Sentinel-1 SAR to inform operational snowpack simulations in alpine areas over large extents. We could demonstrate that a pre-operational version of the snow-hydrological model fsm_preop was well aligned with snow depth observations at hundreds of monitoring sites. However, notable discrepancies were observed between fsm_preop and wet snow maps at the onset of the melting season over a span of five years. For an in-depth performance assessment, we used the wet snow line (WSL) as an aspect-dependent elevation line across which the snowpack transitions from dry to wet snow conditions for a given hydrological unit. This metric provides a spatially aggregated summary of the information obtained from wet snow maps, enabling the exploration of regional variations in moistening dynamics. This aggregation also mitigates data quality issues and data gaps at the pixel level that would hamper model evaluation.

While the simulated WSL matched the observations well in north slopes and flat areas, the model had a substantial dry bias in the south sector, suggesting a delay in the sun-induced melt. Snow lines (SL) derived from Sentinel-2 snow cover fraction retrieval show that this dry bias coincides with a too late seasonal snowpack depletion. Both biases were substantially reduced when an update of the model albedo parametrization was applied. ~~This demonstrates that the wet snow maps contain complementary information for improving snowpack models.~~

Wet snow maps provide valuable information about the snowpack state much earlier in the ablation season than snow cover fraction observations. This is an important asset of WSL data for operational applications. Snow cover fraction observations are much more detailed, but come too late in the season to allow mitigation of biases that arose much earlier during the winter.

Our study demonstrates that wet snow maps and snow cover fraction observations can provide complementary information to those from flat-field snow depth observations, allowing us to evaluate snow-hydrological models from a new perspective. Satellite observations can be used to evaluate the simulations in a diversity of topographic conditions, contrary to flat-field snow depth observations. Finally, as snow depth observations are rare at high elevations, satellite imagery provides a unique opportunity to constrain models particularly at those altitudes.

Code availability. The GitHub repository of FSM2oshd will be made available in the published version of the manuscript.

Author contributions. BC and TJ conceptualized the study. BC performed the simulations and analysed the results with input from TJ. JM and LQ helped with running the simulations. All authors contributed to model development of the OSHD modelling framework and contributed to the manuscript.

Competing interests. The authors have no competing interests to declare.

Acknowledgements. The authors would like to thank Marie Dumont for helpful discussions on the albedo parametrization. This study has been partly funded by the ESA EXPRO+ AlpSnow - Alps Regional Initiative project (Contract No. 4000132770). The OSHD model (FSM2oshd) development and implementation was largely funded by the Swiss Federal Office for the Environment (FOEN).

References

Aalstad, K., Westermann, S., Schuler, T. V., Boike, J., and Bertino, L.: Ensemble-Based Assimilation of Fractional Snow-Covered Area Satellite Retrievals to Estimate the Snow Distribution at Arctic Sites, The Cryosphere, 12, 247–270, https://doi.org/10.5194/tc-12-247-2018, 2018.

Aalstad, K., Westermann, S., and Bertino, L.: Evaluating Satellite Retrieved Fractional Snow-Covered Area at a High-Arctic Site Using Terrestrial Photography, Remote Sensing of Environment, 239, 111 618, https://doi.org/10.1016/j.rse.2019.111618, 2020.

Alonso-González, E., Gutmann, E., Aalstad, K., Fayad, A., Bouchet, M., and Gascoin, S.: Snowpack Dynamics in the Lebanese Mountains from Quasi-Dynamically Downscaled ERA5 Reanalysis Updated by Assimilating Remotely Sensed Fractional Snow-Covered Area, Hydrology and Earth System Sciences, 25, 4455–4471, https://doi.org/10.5194/hess-25-4455-2021, 2021.

Alonso-González, E., Aalstad, K., Pirk, N., Mazzolini, M., Treichler, D., Leclercq, P., Westermann, S., López-Moreno, J. I., and Gascoin, S.: Spatio-Temporal Information Propagation Using Sparse Observations in Hyper-Resolution Ensemble-Based Snow Data Assimilation, Hydrology and Earth System Sciences, 27, 4637–4659, https://doi.org/10.5194/hess-27-4637-2023, 2023.

Andreadis, K. M. and Lettenmaier, D. P.: Assimilating Remotely Sensed Snow Observations into a Macroscale Hydrology Model, Advances in water resources, 29, 872–886, https://doi.org/10.1016/j.advwatres.2005.08.004, 2006.

Baba, M., Gascoin, S., and Hanich, L.: Assimilation of Sentinel-2 Data into a Snowpack Model in the High Atlas of Morocco, Remote Sensing, 10, 1982, https://doi.org/10.3390/rs10121982, 2018.

Barnett, T. P., Adam, J. C., and Lettenmaier, D. P.: Potential Impacts of a Warming Climate on Water Availability in Snow-Dominated Regions, Nature, 438, 303–309, https://doi.org/10.1038/nature04141, 2005.

Baron, M., Haddjeri, A., Lafaysse, M., Le Toumelin, L., Vionnet, V., and Fructus, M.: SnowPappus v1.0, a Blowing-Snow Model for Large-Scale Applications of the Crocus Snow Scheme, Geoscientific Model Development, 17, 1297–1326, https://doi.org/10.5194/gmd-17-1297-2024, 2024.

Barrou Dumont, Z., Gascoin, S., Hagolle, O., Ablain, M., Jugier, R., Salgues, G., Marti, F., Dupuis, A., Dumont, M., and Morin, S.: Brief Communication: Evaluation of the Snow Cover Detection in the Copernicus High Resolution Snow & Ice Monitoring Service, The Cryosphere, 15, 4975–4980, https://doi.org/10.5194/tc-15-4975-2021, 2021.

Brauchli, T., Trujillo, E., Huwald, H., and Lehning, M.: Influence of Slope-Scale Snowmelt on Catchment Response Simulated With the *Alpine3D* Model, Water Resources Research, 53, 10 723–10 739, https://doi.org/10.1002/2017WR021278, 2017.

Buchelt, S., Skov, K., Rasmussen, K. K., and Ullmann, T.: Sentinel-1 Time Series for Mapping Snow Cover Depletion and Timing of Snowmelt in Arctic Periglacial Environments: Case Study from Zackenberg and Kobbefjord, Greenland, The Cryosphere, 16, 625–646, https://doi.org/10.5194/tc-16-625-2022, 2022.

Buchhorn, M.: Copernicus Global Land Service: Global Biome Cluster Layer for the 100m Global Land Cover Processing Line, https://doi.org/10.5281/zenodo.5848610, 2022.

Cluzet, B., Revuelto, J., Lafaysse, M., Tuzet, F., Cosme, E., Picard, G., Arnaud, L., and Dumont, M.: Towards the Assimilation of Satellite Reflectance into Semi-Distributed Ensemble Snowpack Simulations, Cold Regions Science and Technology, 170, 102 918, https://doi.org/10.1016/j.coldregions.2019.102918, 2020.

Cluzet, B., Lafaysse, M., Cosme, E., Albergel, C., Meunier, L.-F., and Dumont, M.: CrocO_v1.0: A Particle Filter to Assimilate Snowpack Observations in a Spatialised Framework, Geoscientific Model Development, 14, 1595–1614, https://doi.org/10.5194/gmd-14-1595-2021, 2021.

Cluzet, B., Lafaysse, M., Deschamps-Berger, C., Vernay, M., and Dumont, M.: Propagating Information from Snow Observations with CrocO Ensemble Data Assimilation System: A 10-Years Case Study over a Snow Depth Observation Network, The Cryosphere, 16, 1281–1298, https://doi.org/10.5194/tc-16-1281-2022, 2022.

Cristea, N. C., Bennett, A., Nijssen, B., and Lundquist, J. D.: When and Where Are Multiple Snow Layers Important for Simulations of Snow Accumulation and Melt?, Water Resources Research, 58, e2020WR028 993, https://doi.org/10.1029/2020WR028993, 2022.

De Lannoy, G. J. M., Reichle, R. H., Arsenault, K. R., Houser, P. R., Kumar, S., Verhoest, N. E. C., and Pauwels, V. R. N.: Multiscale Assimilation of Advanced Microwave Scanning Radiometer–EOS Snow Water Equivalent and Moderate Resolution Imaging Spectroradiometer Snow Cover Fraction Observations in Northern Colorado, Water Resources Research, 48, https://doi.org/10.1029/2011wr010588, 2012.

Diffenbaugh, N. S., Scherer, M., and Ashfaq, M.: Response of Snow-Dependent Hydrologic Extremes to Continued Global Warming, Nature Climate Change, 3, 379–384, https://doi.org/10.1038/nclimate1732, 2013.

Dingman, S. L.: Physical Hydrology: Third Edition, Waveland Press, 2015.

Douville, H., Royer, J. F., and Mahfouf, J. F.: A New Snow Parameterization for the Météo-France Climate Model: Part I: Validation in Stand-Alone Experiments, Climate Dynamics, 12, 21–35, https://doi.org/10.1007/BF00208760, 1995.

Dujardin, J. and Lehning, M.: Wind-Topo: Downscaling Near-surface Wind Fields to High-resolution Topography in Highly Complex Terrain with Deep Learning, Quarterly Journal of the Royal Meteorological Society, 148, 1368–1388, https://doi.org/10.1002/qj.4265, 2022.

Essery, R.: A Factorial Snowpack Model (FSM 1.0), Geosci. Model Dev., 8, 3867–3876, https://doi.org/10.5194/gmd-8-3867-2015, 2015.

Essery, R., Morin, S., Lejeune, Y., and Bauduin-Ménard, C.: A Comparison of 1701 Snow Models Using Observations from an Alpine Site, Adv. Water Res., 55, 131–148, https://doi.org/10.1016/j.advwatres.2012.07.013, 2013.

Fiddes, J., Aalstad, K., and Westermann, S.: Hyper-Resolution Ensemble-Based Snow Reanalysis in Mountain Regions Using Clustering, Hydrology and Earth System Sciences, 23, 4717–4736, https://doi.org/10.5194/hess-23-4717-2019, 2019.

Freudiger, D., Kohn, I., Seibert, J., Stahl, K., and Weiler, M.: Snow Redistribution for the Hydrological Modeling of Alpine Catchments, WIREs Water, 4, e1232, https://doi.org/10.1002/wat2.1232, 2017.

Gardner, A. S. and Sharp, M. J.: A Review of Snow and Ice Albedo and the Development of a New Physically Based Broadband Albedo Parametrization, J. Geophys. Res., 115, F01 009, https://doi.org/10.1029/2009JF001444, 2010.

Gaudard, L., Romerio, F., Dalla Valle, F., Gorret, R., Maran, S., Ravazzani, G., Stoffel, M., and Volonterio, M.: Climate Change Impacts on Hydropower in the Swiss and Italian Alps, Science of the Total Environment, 493, 1211–1221, https://doi.org/10.1016/j.scitotenv.2013.10.012, 2014.

Griessinger, N., Schirmer, M., Helbig, N., Winstral, A., Michel, A., and Jonas, T.: Implications of Observation-Enhanced Energy-Balance Snowmelt Simulations for Runoff Modeling of Alpine Catchments, Advances in Water Resources, 133, 103 410, https://doi.org/10.1016/j.advwatres.2019.103410, 2019.

Grünewald, T. and Lehning, M.: Are Flat-Field Snow Depth Measurements Representative? A Comparison of Selected Index Sites with Areal Snow Depth Measurements at the Small Catchment Scale, Hydrological Processes, 29, 1717–1728, https://doi.org/10.1002/hyp.10295, 2015.

Guiot, A., Karbou, F., James, G., and Durand, P.: Insights into Segmentation Methods Applied to Remote Sensing SAR Images for Wet Snow Detection, Geosciences, 13, 193, https://doi.org/10.3390/geosciences13070193, 2023.

Gupta, R. P.: Dry and Wet Snow Line/Zone, in: Encyclopedia of Snow, Ice and Glaciers, edited by Singh, V. P., Singh, P., and Haritashya, U. K., Encyclopedia of Earth Sciences Series, pp. 240–241, Springer Netherlands, Dordrecht, https://doi.org/10.1007/978-90-481-2642-2_125, 2011.

Helbig, N., Schirmer, M., Magnusson, J., Mäder, F., van Herwijnen, A., Quéno, L., Bühler, Y., Deems, J. S., and Gascoin, S.: A Seasonal

560   Algorithm of the Snow-Covered Area Fraction for Mountainous Terrain, The Cryosphere, 15, 4607–4624, https://doi.org/10.5194/tc-15-4607-2021, 2021.

Isotta, F. A., Frei, C., Weilguni, V., Perčec Tadić, M., Lassègues, P., Rudolf, B., Pavan, V., Cacciamani, C., Antolini, G., Ratto, S. M., Munari, M., Micheletti, S., Bonati, V., Lussana, C., Ronchi, C., Panettieri, E., Marigo, G., and Vertačnik, G.: The Climate of Daily Precipitation in the Alps: Development and Analysis of a High-Resolution Grid Dataset from Pan-Alpine Rain-Gauge Data, International Journal of

565   Climatology, 34, 1657–1675, https://doi.org/10.1002/joc.3794, 2014.

Jonas, T., Webster, C., Mazzotti, G., and Malle, J.: HPEval: A Canopy Shortwave Radiation Transmission Model Using High-Resolution Hemispherical Images, Agricultural and Forest Meteorology, 284, 107 903, https://doi.org/10.1016/j.agrformet.2020.107903, 2020.

Karbou, F., Veyssière, G., Coleou, C., Dufour, A., Gouttevin, I., Durand, P., Gascoin, S., and Grizonnet, M.: Monitoring Wet Snow Over an Alpine Region Using Sentinel-1 Observations, Remote Sensing, 13, 381, https://doi.org/10.3390/rs13030381, 2021.

570   Karbou, F., James, G., Fructus, M., and Marti, F.: On the Evaluation of the SAR-Based Copernicus Snow Products in the French Alps, Geosciences, 12, 420, https://doi.org/10.3390/geosciences12110420, 2022.

Keuris, L., Hetzenecker, M., Nagler, T., Mölg, N., and Schwaizer, G.: An Adaptive Method for the Estimation of Snow-Covered Fraction with Error Propagation for Applications from Local to Global Scales, Remote Sensing, 15, 1231, https://doi.org/10.3390/rs15051231, 2023.

575   Krinner, G., Derksen, C., Essery, R., Flanner, M., Hagemann, S., Clark, M., Hall, A., Rott, H., Brutel-Vuilmet, C., Kim, H., Ménard, C. B., Mudryk, L., Thackeray, C., Wang, L., Arduini, G., Balsamo, G., Bartlett, P., Boike, J., Boone, A., Chéruy, F., Colin, J., Cuntz, M., Dai, Y., Decharme, B., Derry, J., Ducharne, A., Dutra, E., Fang, X., Fierz, C., Ghattas, J., Gusev, Y., Haverd, V., Kontu, A., Lafaysse, M., Law, R., Lawrence, D., Li, W., Marke, T., Marks, D., Ménégoz, M., Nasonova, O., Nitta, T., Niwano, M., Pomeroy, J., Raleigh, M. S., Schaedler, G., Semenov, V., Smirnova, T. G., Stacke, T., Strasser, U., Svenson, S., Turkov, D., Wang, T., Wever, N., Yuan, H., Zhou, W., and Zhu,

580   D.: ESM-SnowMIP: Assessing Snow Models and Quantifying Snow-Related Climate Feedbacks, Geoscientific Model Development, 11, 5027–5049, https://doi.org/10.5194/gmd-11-5027-2018, 2018.

Lafaysse, M., Hingray, B., Mezghani, A., Gailhard, J., and Terray, L.: Internal Variability and Model Uncertainty Components in Future Hydrometeorological Projections: The Alpine Durance Basin, Water resources research, 50, 3317–3341, https://doi.org/10.1002/2013WR014897, 2014.

585   Lamare, M., Dumont, M., Picard, G., Larue, F., Tuzet, F., Delcourt, C., and Arnaud, L.: Simulating Optical Top-of-Atmosphere Radiance Satellite Images over Snow-Covered Rugged Terrain, The Cryosphere, 14, 3995–4020, https://doi.org/10.5194/tc-14-3995-2020, 2020.

Largeron, C., Dumont, M., Morin, S., Boone, A., Lafaysse, M., Metref, S., Cosme, E., Jonas, T., Winstral, A., and Margulis, S. A.: Toward Snow Cover Estimation in Mountainous Areas Using Modern Data Assimilation Methods: A Review, Frontiers in Earth Science, 8, https://doi.org/10.3389/feart.2020.00325, 2020.

590   Liston, G. E. and Sturm, M.: A Snow-Transport Model for Complex Terrain, Journal of Glaciology, 44, 498–516, https://doi.org/10.1017/S0022143000002021, 1998.

Lund, J., Forster, R. R., Deeb, E. J., Liston, G. E., Skiles, S. M., and Marshall, H.-P.: Interpreting Sentinel-1 SAR Backscatter Signals of Snowpack Surface Melt/Freeze, Warming, and Ripening, through Field Measurements and Physically-Based SnowModel, Remote Sensing, 14, 4002, https://doi.org/10.3390/rs14164002, 2022.

595   Lundquist, J. D. and Dettinger, M. D.: How Snowpack Heterogeneity Affects Diurnal Streamflow Timing, Water Resources Research, 41, https://doi.org/10.1029/2004WR003649, 2005.

Magand, C., Ducharne, A., Le Moine, N., and Gascoin, S.: Introducing Hysteresis in Snow Depletion Curves to Improve the Water Budget of a Land Surface Model in an Alpine Catchment, Journal of hydrometeorology, 15, 631–649, https://doi.org/10.1175/JHM-D-13-091.1, 2014.

600   Magnusson, J., Gustafsson, D., Hüsler, F., and Jonas, T.: Assimilation of Point SWE Data into a Distributed Snow Cover Model Comparing Two Contrasting Methods, Water Resources Research, 50, 7816–7835, https://doi.org/10.1002/2014WR015302, 2014.

Magnusson, J., Wever, N., Essery, R., Helbig, N., Winstral, A., and Jonas, T.: Evaluating Snow Models with Varying Process Representations for Hydrological Applications, Water Resources Research, 51, 2707–2723, https://doi.org/10.1002/2014WR016498, 2015.

Malnes, E., Buanes, A., Nagler, T., Bippus, G., Gustafsson, D., Schiller, C., Metsämäki, S., Pulliainen, J., Luojus, K., Larsen, H. E., Solberg,
605   R., Diamandi, A., and Wiesmann, A.: User Requirements for the Snow and Land Ice Services – CryoLand, The Cryosphere, 9, 1191–1202, https://doi.org/10.5194/tc-9-1191-2015, 2015.

Margulis, A., Cortés, G., Girotto, M., and Durand, M.: A Landsat-Era Sierra Nevada Snow Reanalysis (1985–2015), Journal of Hydrometeorology, 17, 1203–1221, https://doi.org/10.1175/JHM-D-15-0177.1, 2016.

Margulis, S. A., Girotto, M., Cortés, G., and Durand, M.: A Particle Batch Smoother Approach to Snow Water Equivalent Estimation, Journal
610   of Hydrometeorology, 16, 1752–1772, https://doi.org/10.1175/JHM-D-14-0177.1, 2015.

Marin, C., Bertoldi, G., Premier, V., Callegari, M., Brida, C., Hürkamp, K., Tschiersch, J., Zebisch, M., and Notarnicola, C.: Use of Sentinel-1 Radar Observations to Evaluate Snowmelt Dynamics in Alpine Regions., The Cryosphere, 14, 935–935, https://doi.org/10.5194/tc-14-935-2020, 2020.

Marsh, C. B., Pomeroy, J. W., and Wheater, H. S.: The Canadian Hydrological Model (CHM) v1. 0: A Multi-Scale, Multi-Extent, Variable-
615   Complexity Hydrological Model-Design and Overview., Geoscientific Model Development, 13, 225–225, https://doi.org/10.5194/gmd-13-225-2020, 2020.

Mary, A., Dumont, M., Dedieu, J.-P., Durand, Y., Sirguey, P., Milhem, H., Mestre, O., Negi, H. S., Kokhanovsky, A. A., Lafaysse, M., and Morin, S.: Intercomparison of Retrieval Algorithms for the Specific Surface Area of Snow from Near-Infrared Satellite Data in Mountainous Terrain, and Comparison with the Output of a Semi-Distributed Snowpack Model, The Cryosphere, 7, 741–761,
620   https://doi.org/10.5194/tc-7-741-2013, 2013.

Mätzler, C.: Applications of the Interaction of Microwaves with the Natural Snow Cover, Remote Sensing Reviews, 2, 259–387, https://doi.org/10.1080/02757258709532086, 1987.

Mott, R., Egli, L., Grünewald, T., Dawes, N., Manes, C., Bavay, M., and Lehning, M.: Micrometeorological Processes Driving Snow Ablation in an Alpine Catchment, The Cryosphere, 5, 1083–1098, https://doi.org/10.5194/tc-5-1083-2011, 2011.

625   Mott, R., Vionnet, V., and Grünewald, T.: The Seasonal Snow Cover Dynamics: Review on Wind-Driven Coupling Processes, Frontiers in Earth Science, 6, https://doi.org/10.3389/feart.2018.00197, 2018.

Mott, R., Winstral, A., Cluzet, B., Helbig, N., Magnusson, J., Mazzotti, G., Quéno, L., Schirmer, M., Webster, C., and Jonas, T.: Operational Snow-Hydrological Modeling for Switzerland, Frontiers in Earth Science, 11, 1228 158, https://doi.org/10.3389/feart.2023.1228158, 2023.

630   Nagler, T., Rott, H., Ripper, E., Bippus, G., and Hetzenecker, M.: Advancements for Snowmelt Monitoring by Means of Sentinel-1 SAR, Remote Sensing, 8, 348, https://doi.org/10.3390/rs8040348, 2016.

Oberrauch, M., Cluzet, B., Magnusson, J., and Jonas, T.: Improving Fully Fistributed Snowpack Simulations by Mapping Perturbations of Meteorological Forcings Fnferred from Particle Filter Assimilation of Snow Monitoring Data, Water Resources Research, in press.

Parajka, J., Pepe, M., Rampini, A., Rossi, S., and Blöschl, G.: A Regional Snow-Line Method for Estimating Snow Cover from MODIS during Cloud Cover, Journal of Hydrology, 381, 203–212, https://doi.org/10.1016/j.jhydrol.2009.11.042, 2010.

Qin, Y., Abatzoglou, J. T., Siebert, S., Huning, L. S., AghaKouchak, A., Mankin, J. S., Hong, C., Tong, D., Davis, S. J., and Mueller, N. D.: Agricultural Risks from Changing Snowmelt, Nature Climate Change, 10, 459–465, https://doi.org/10.1038/s41558-020-0746-8, 2020.

Quéno, L., Fierz, C., van Herwijnen, A., Longridge, D., and Wever, N.: Deep Ice Layer Formation in an Alpine Snowpack: Monitoring and Modeling, The Cryosphere, 14, 3449–3464, https://doi.org/10.5194/tc-14-3449-2020, 2020.

Quéno, L., Mott, R., Morin, P., Cluzet, B., Mazzotti, G., and Jonas, T.: Snow Redistribution in an Intermediate-Complexity Snow Hydrology Modelling Framework, Preprint, Snow/Numerical Modelling, https://doi.org/10.5194/egusphere-2023-2071, 2023.

Raleigh, M. S., Lundquist, J. D., and Clark, M. P.: Exploring the Impact of Forcing Error Characteristics on Physically Based Snow Simulations within a Global Sensitivity Analysis Framework, Hydrology and Earth System Sciences, 19, 3153–3179, https://doi.org/10.5194/hess-19-3153-2015, 2015.

Scipión, D. E., Mott, R., Lehning, M., Schneebeli, M., and Berne, A.: Seasonal Small-Scale Spatial Variability in Alpine Snowfall and Snow Accumulation, Water Resources Research, 49, 1446–1457, https://doi.org/10.1002/wrcr.20135, 2013.

Techel, F. and Pielmeier, C.: Point Observations of Liquid Water Content in Wet Snow – Investigating Methodical, Spatial and Temporal Aspects, The Cryosphere, 5, 405–418, https://doi.org/10.5194/tc-5-405-2011, 2011.

Vernay, M., Lafaysse, M., Monteiro, D., Hagenmuller, P., Nheili, R., Samacoïts, R., Verfaillie, D., and Morin, S.: The S2M Meteorological and Snow Cover Reanalysis over the French Mountainous Areas: Description and Evaluation (1958–2021), Earth System Science Data, 14, 1707–1733, https://doi.org/10.5194/essd-14-1707-2022, 2022.

Veyssière, G., Karbou, F., Morin, S., Lafaysse, M., and Vionnet, V.: Evaluation of Sub-Kilometric Numerical Simulations of C-Band Radar Backscatter over the French Alps against Sentinel-1 Observations, Remote Sensing, 11, https://doi.org/10.3390/rs11010008, 2019.

Vionnet, V., Marsh, C. B., Menounos, B., Gascoin, S., Wayand, N. E., Shea, J., Mukherjee, K., and Pomeroy, J. W.: Multi-Scale Snowdrift-Permitting Modelling of Mountain Snowpack, The Cryosphere, 15, 743–769, https://doi.org/10.5194/tc-15-743-2021, 2021.

Vögeli, C., Lehning, M., Wever, N., and Bavay, M.: Scaling Precipitation Input to Spatially Distributed Hydrological Models by Measured Snow Distribution, Frontiers in Earth Science, 4, 2016.

Wever, N., Fierz, C., Mitterer, C., Hirashima, H., and Lehning, M.: Solving Richards Equation for Snow Improves Snowpack Meltwater Runoff Estimations in Detailed Multi-Layer Snowpack Model, The Cryosphere, 8, 257–274, https://doi.org/10.5194/tc-8-257-2014, 2014.

Winstral, A., Magnusson, J., Schirmer, M., and Jonas, T.: The Bias-Detecting Ensemble: A New and Efficient Technique for Dynamically Incorporating Observations Into Physics-Based, Multilayer Snow Models, Water Resources Research, 55, 613–631, https://doi.org/10.1029/2018WR024521, 2019.

Würzer, S., Wever, N., Juras, R., Lehning, M., and Jonas, T.: Modelling Liquid Water Transport in Snow under Rain-on-Snow Conditions – Considering Preferential Flow, Hydrology and Earth System Sciences, 21, 1741–1756, https://doi.org/10.5194/hess-21-1741-2017, 2017.
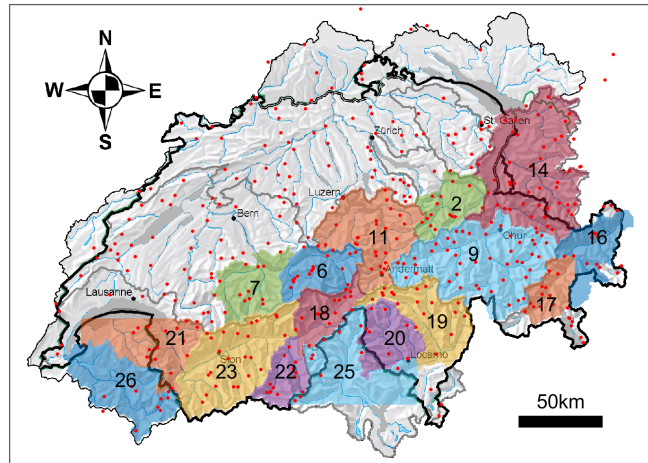
Figure 1. Map of the model domain, with the identifier of hydrological units ~~marked~~(MEZ), and locations of the snow stations (red points). Switzerland's border is denoted by the thick black line.
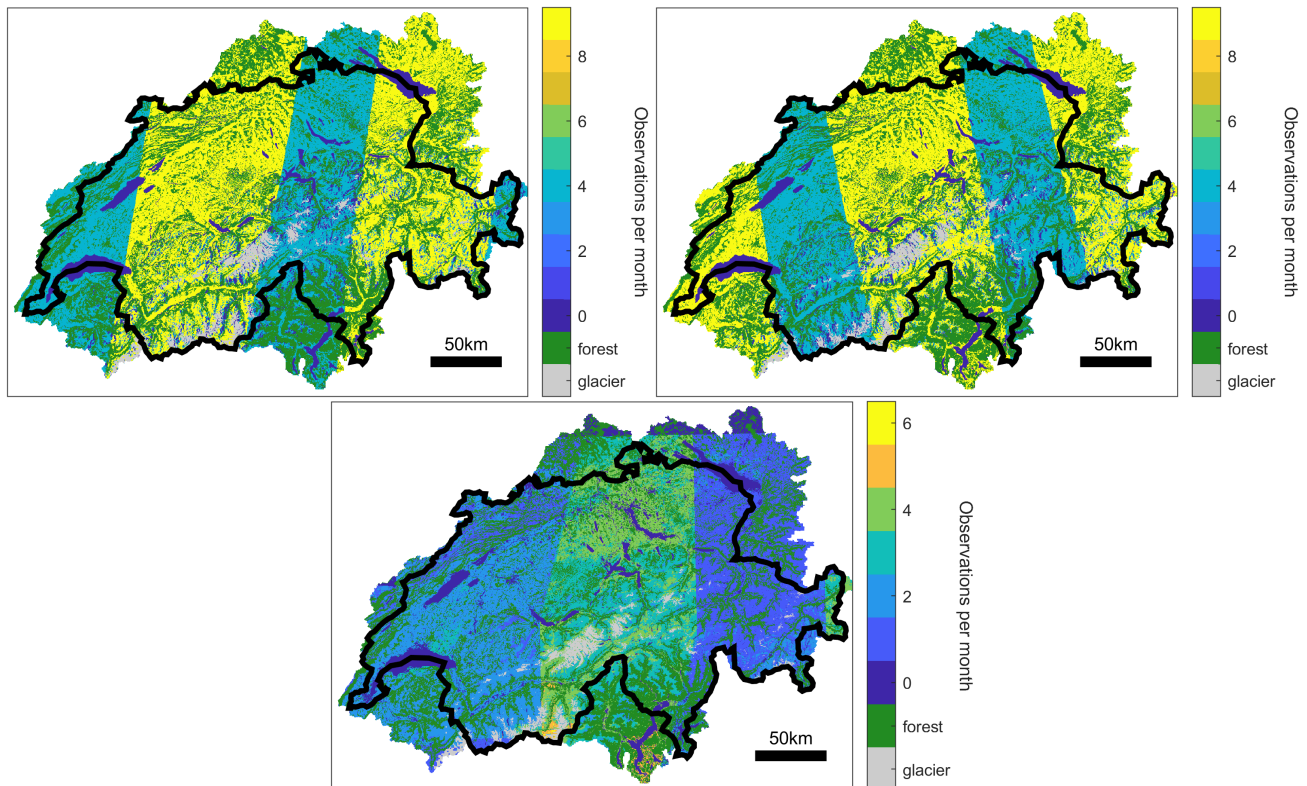
Figure 2. Sentinel-1 05UTC (top left) and 17UTC (top right), and Sentinel-2 (bottom), number of valid observations per month and per pixel over the whole period. Forest and glaciers have been masked out. Switzerland national borders are indicated in black.
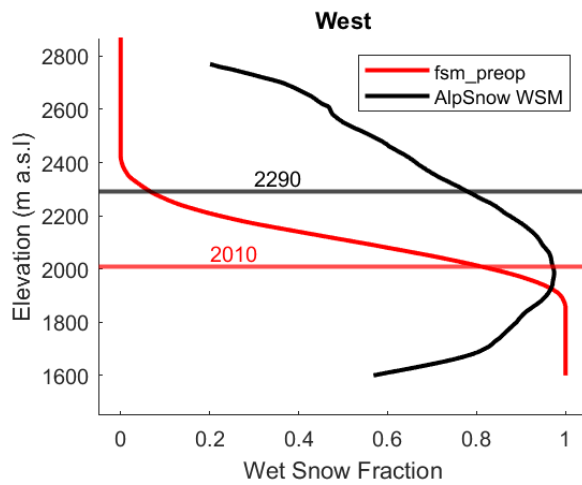
Figure 3. Computation of the wet snow line, for fsm_preop and AlpSnow data, in this example for westerly aspects (247.5-292.5°N) of MEZ 11 on 2019-04-01, 17UTC.
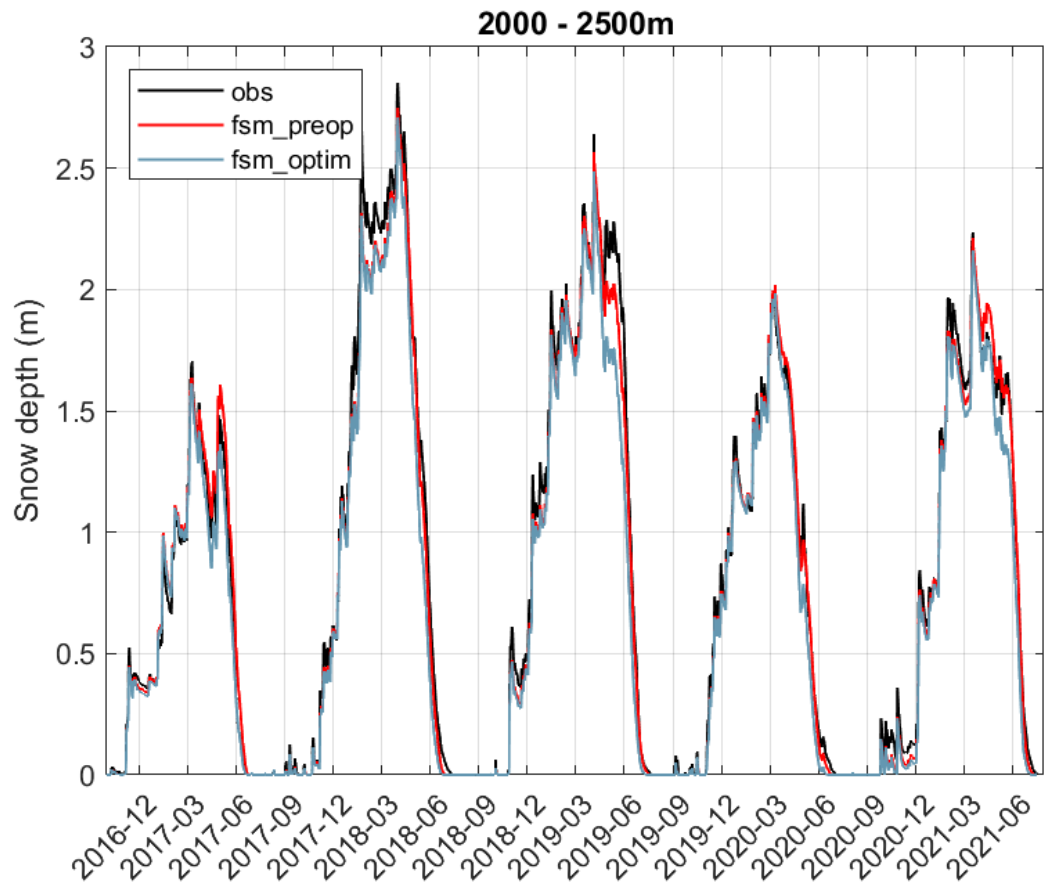
Figure 4. Average of fsm_preop (red), fsm_optim (light blue), and flat-field snow-depth observations (black) over the full study domain in the elevation range 2000–2500 m a.s.l.
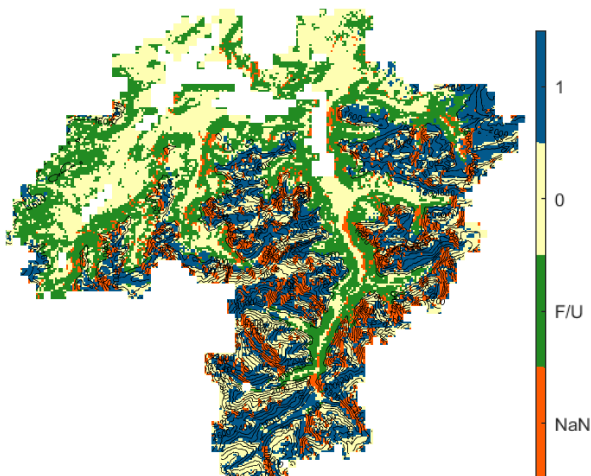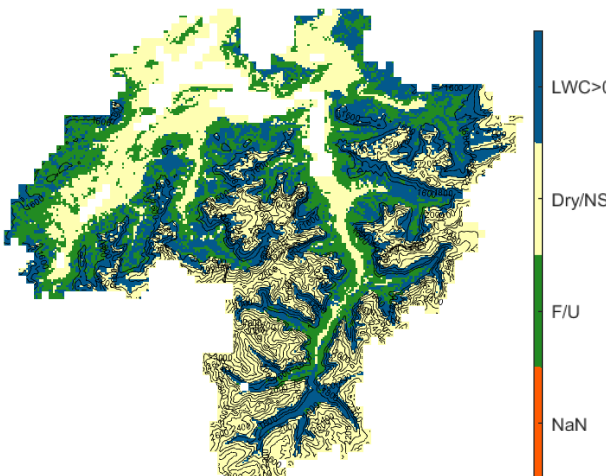
(a) observation   (b) fsm_preop

Figure 5. Sentinel-1 250m wet snow map (a) and simulated presence of liquid water using fsm_preop (b) for MEZ 11 on 2019-04-01, 17UTC. Blue denotes wet snow, light yellow dry conditions (or no snow/patchy snow), green forest and urban pixels, and orange denotes missing data due to geometric distortions in the observation. Lakes and pixels outside of MEZ 11 are masked out.

(a) aggregated observations   (b) aggregated fsm_preop   (c) aggregated fsm_optim
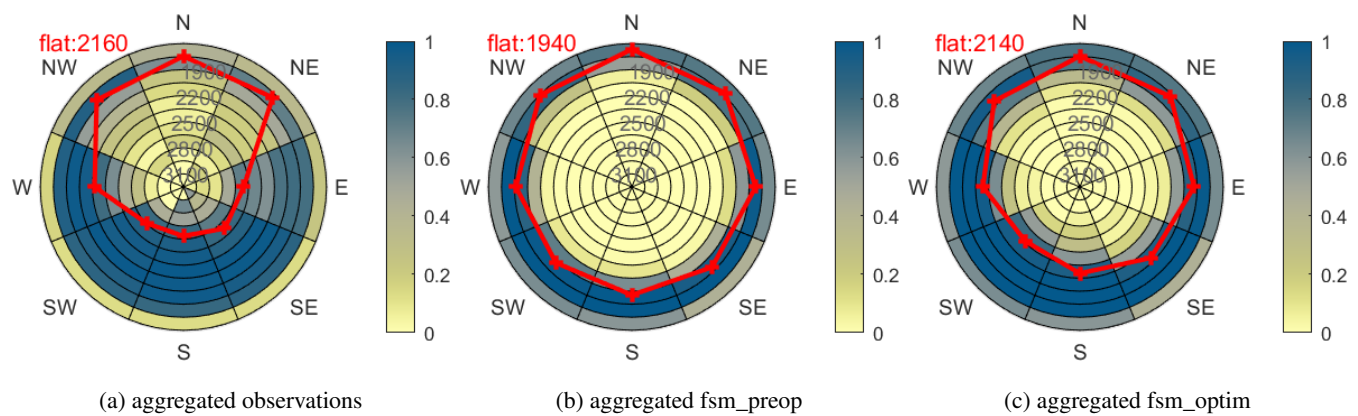
Figure 6. Fraction of wet snow pixels by 150m elevation bands and 8 aspect classes, from AlpSnow WSM (a) fsm_preop (b), and fsm_optim (c) over MEZ 11. The wet snow line is displayed in red, and its altitude in flat terrain is indicated in the top left of each panel.
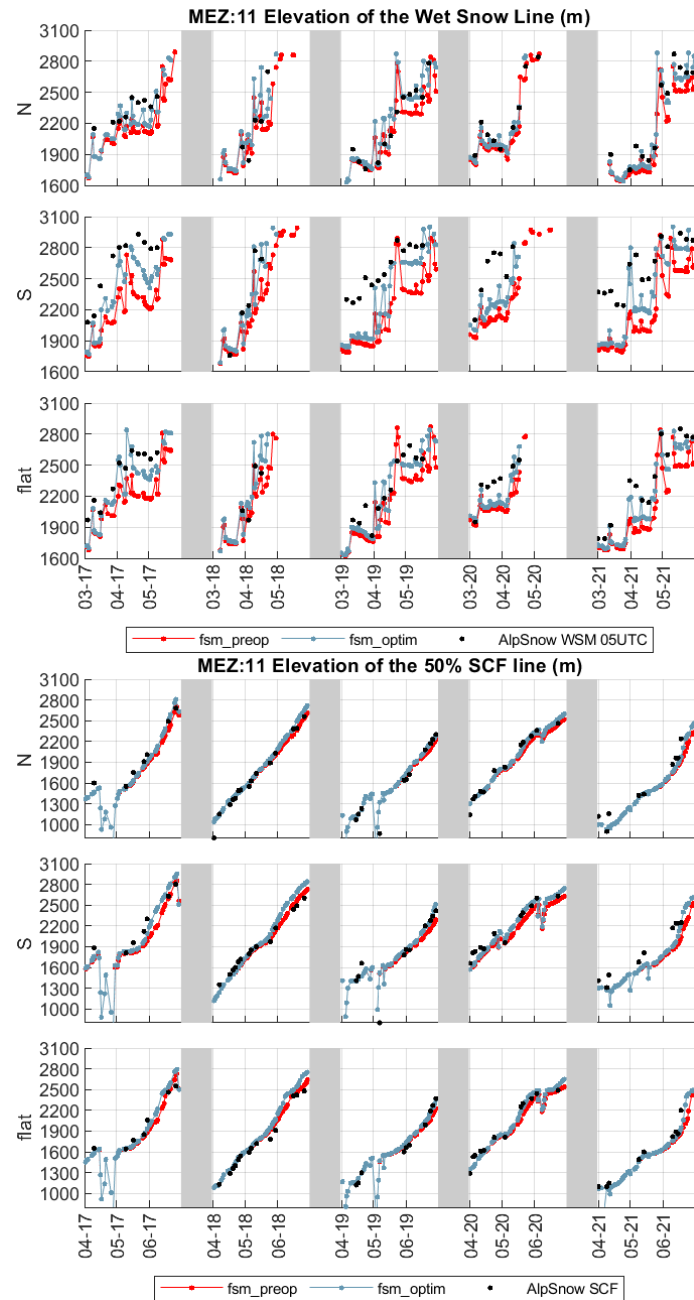
Figure 7. Time series of wet snow line (top panel) in the observations (black), fsm_preop (red) and fsm_optim (light blue) and snow lines (bottom panel) for the different aspects and seasons in MEZ 11. Only descending (05 UTC) Sentinel-1 tracks were used to determine the WSL.
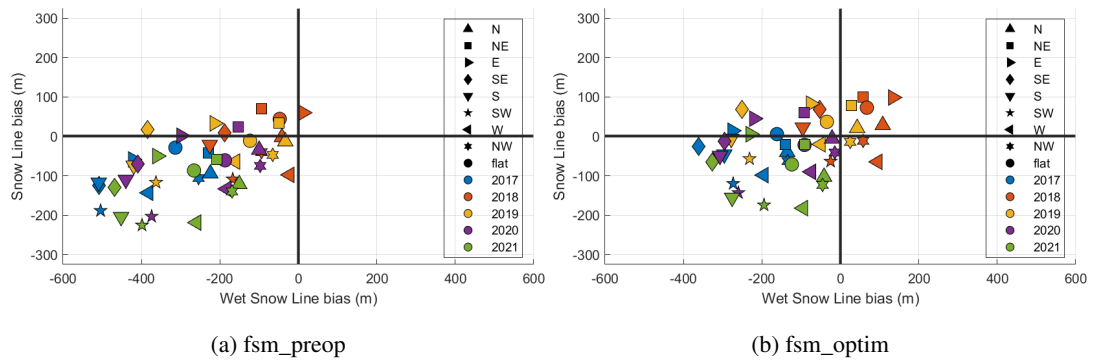
Figure 8. Snow line bias as a function of wet snow line bias (at 05UTC) for MEZ 11, across years and aspects.
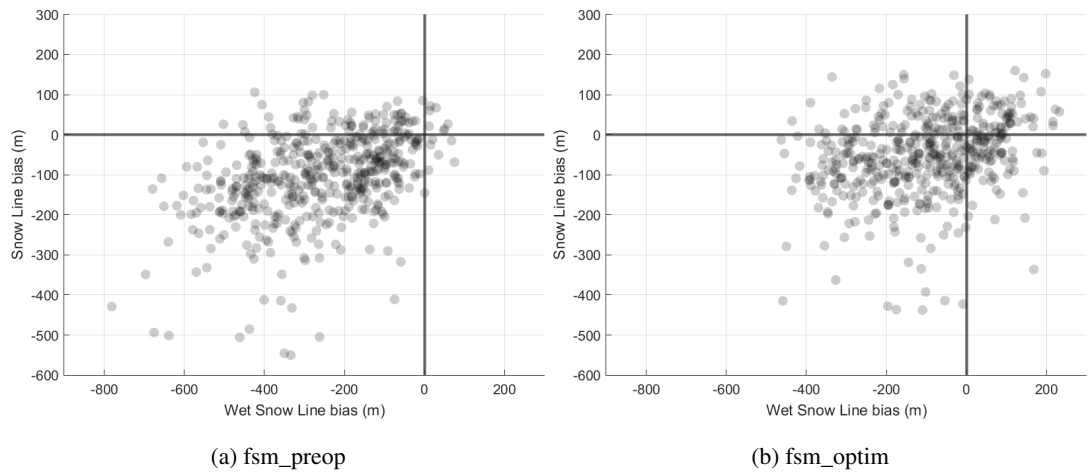
Figure 9. Snow line bias as a function of wet snow line bias (at 05UTC) for all MEZ, across years and aspects.

 Appendix A: **Complementary figures**
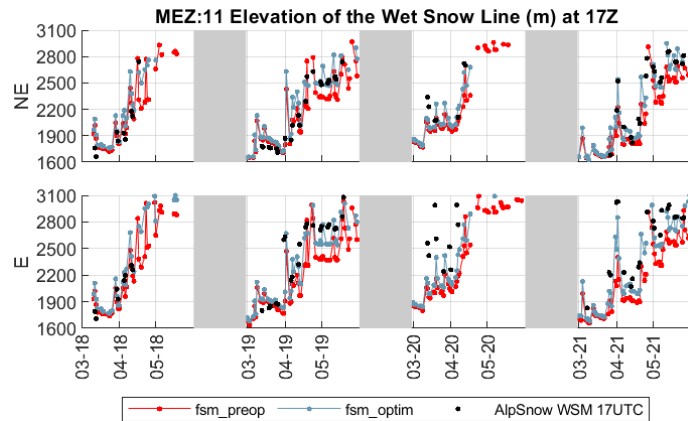
Figure A1. Time series of wet snow line in the observations (black), fsm_preop (red) and fsm_optim (light blue) for the different aspects and seasons in MEZ 11. Only ascending (17 UTC) Sentinel-1 tracks were used to determine the WSL. Note that for technical reasons, year 2017 is not represented, as no model output were saved for this year at 17UTC.